JOURNAL OF GEOPHYSICAL RESEARCH, VOL. 112, B03308, doi:10.1029/2006JB004632, 2007

Click Here for Full Article

Forecast experiment: Do temporal and spatial *b* value variations along the Calaveras fault portend $M \geq 4.0$ earthquakes?

Tom Parsons[1]

Received 14 July 2006; revised 16 October 2006; accepted 30 October 2006; published 28 March 2007.

[1] The power law distribution of earthquake magnitudes and frequencies is a fundamental scaling relationship used for forecasting. However, can its slope (*b* value) be used on individual faults as a stress indicator? Some have concluded that *b* values drop just before large shocks. Others suggested that temporally stable low *b* value zones identify future large-earthquake locations. This study assesses the frequency of *b* value anomalies portending $M \geq 4.0$ shocks versus how often they do not. I investigated $M \geq 4.0$ Calaveras fault earthquakes because there have been 25 over the 37-year duration of the instrumental catalog on the most active southern half of the fault. With that relatively large sample, I conducted retrospective time and space earthquake forecasts. I calculated temporal *b* value changes in 5-km-radius cylindrical volumes of crust that were significant at 90% confidence, but these changes were poor forecasters of $M \geq 4.0$ earthquakes. $M \geq 4.0$ events were as likely to happen at times of high *b* values as they were at low ones. However, I could not rule out a hypothesis that spatial *b* value anomalies portend $M \geq 4.0$ events; of 20 $M \geq 4$ shocks that could be studied, 6 to 8 (depending on calculation method) occurred where *b* values were significantly less than the spatial mean, 1 to 2 happened above the mean, and 10 to 13 occurred within 90% confidence intervals of the mean and were thus inconclusive. Thus spatial *b* value variation might be a useful forecast tool, but resolution is poor, even on seismically active faults.

Citation: Parsons, T. (2007), Forecast experiment: Do temporal and spatial *b* value variations along the Calaveras fault portend $M \geq 4.0$ earthquakes?, *J. Geophys. Res.*, *112*, B03308, doi:10.1029/2006JB004632.

1. Introduction

[2] Regional earthquake magnitudes are distributed in a power law, as [*Ishimoto and Iida*, 1939; *Gutenberg and Richter*, 1954]

$$\log_{10}(N_M) = a - bM \tag{1}$$

This observation has long intrigued seismologists because, if it holds over a broad range of earthquake magnitudes, it can predict large earthquake frequency from a distribution of small earthquakes by extrapolating the *b* value, or slope of the linear distribution. Knowledge of large earthquake frequency is of course needed for forecasting.

[3] Extrapolation of a magnitude-frequency distribution may lead to an expected regional large earthquake rate, but we usually want more specificity. Motivated by laboratory experiments [*Scholz*, 1968; *Amitrano*, 2003], theoretical studies [e.g., *Main et al.*, 1992], and observations [*Schorlemmer et al.*, 2005] showing *b* values decreasing with increasing stress, investigators have sought temporal and/or spatial *b* value variations that correlate with earthquake occurrence. Two viewpoints prevail: in the first, time-varying *b* values are associated with large earthquakes or moment rate changes [e.g., *Imoto*, 1991; *Kebede and Kulhánek*, 1994; *Sahu and Saikia*, 1994; *Enescu and Ito*, 2001; *Cao and Gao*, 2002; *Ziv et al.*, 2003; *Nuannin et al.*, 2005]. In the second, *b* values are found constant in time, but spatial variations are related to earthquake occurrence and/or likelihood [*Abercrombie and Brune*, 1994; *Westerhaus et al.*, 2002; *Schorlemmer et al.*, 2003; *Wyss et al.*, 2004; *Schorlemmer et al.*, 2004; *Wyss and Stefansson*, 2006]. Associations between large earthquakes and *b* value variation are thus often noted. Accompanying catalogs of earthquakes not associated with *b* value changes, or *b* value changes not associated with large earthquakes are lacking however. To assess *b* value variations as a forecast tool, it is important to know failure rates as well as success rates.

[4] In this paper I conduct a retrospective forecast experiment using time and space distributions of $2.0 \geq M < 4.0$ earthquakes on the Calaveras fault, a spur of the San Andreas fault system located in the San Francisco Bay region of California (Figure 1). The purpose is to test whether $M \geq 4.0$ Calaveras fault earthquakes that happened between 1968 and 2006 showed any relation to either temporal or spatial *b* value variations. I chose the Calaveras fault for study because it has energetic microseismicity and has had 25 moderate-sized ($4.0 \geq M \leq 6.2$) earthquakes since 1968. A large sample of moderate earthquakes all

[1]U.S. Geological Survey, Menlo Park, California, USA.

This paper is not subject to U.S. copyright.
Published in 2007 by the American Geophysical Union.

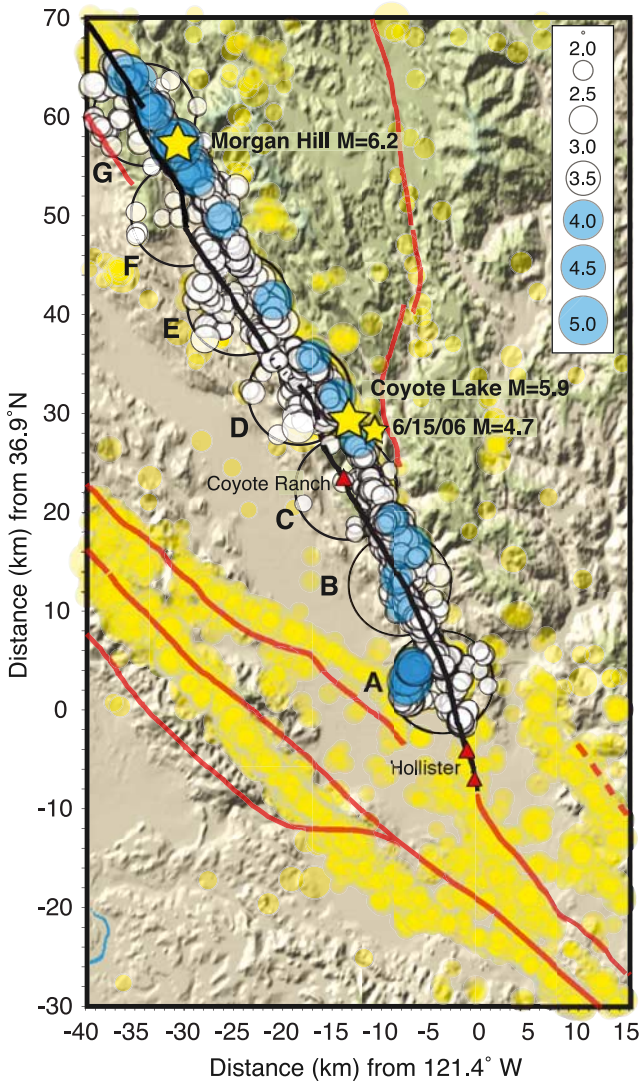

Figure 1. Map showing the investigated segment of the Calaveras fault, the trace of which is black; other regional faults are shown as red lines. Subcatalogs used for the temporal forecast test are earthquakes within vertical cylinders identified by circles labeled A–G. Earthquakes used for temporal and spatial forecast tests are shown by white circles, have a magnitude range of $2.0 \leq M < 4.0$, and occurred between 1968 and 2005. Blue circles show $M \geq 4.0$ earthquakes for which forecasts were attempted. Regional seismicity not used in this study is shown with yellow circles. Notable earthquakes like the 1979 $M = 5.8$ Coyote Lake, and 1984 $M = 6.2$ Morgan Hill events are shown with yellow stars, as is the 15 June 2006 $M = 4.7$ shock that occurred during this study. Sites with long-term creep observations are labeled and identified with red triangles.

from the same fault, and thus same tectonic setting, offers a testing opportunity of hypotheses that time and/or space varying *b* values portend future earthquakes. A disadvantage is that observations from $M\sim4$ to $M\sim6$ earthquakes may not scale to the largest events most important in hazard assessments. However, $M\sim4$ earthquakes have features in common with larger shocks in terms of scaling relations like energy release to moment [e.g., *McGarr*, 1999; *Kanamori and Heaton*, 2000; *Scholz*, 2002]; thus results presented here might reasonably be extrapolated to larger earthquakes.

[5] After brief summaries of the geologic setting of the Calaveras fault, earthquake catalogs, and methodology, this paper discusses whether there are significant temporal *b* value variations. Upon identifying these, an attempt to relate them to $M \geq 4$ earthquake occurrence is undertaken. Then the alternative hypothesis is examined; assuming that *b* values are stationary in time, spatial *b* value calculations are made for the Calaveras fault representing conditions prior to each $M \geq 4$ earthquake time, and *b* values at the hypocenters are compared with the distribution along the whole fault.

2. Geologic Setting

[6] The San Francisco Bay region is sliced by a series of near-vertical right-lateral strike-slip faults of the San Andreas system. About 30–40 mm/yr of plate boundary deformation is accommodated by this subparallel fault set [*DeMets et al.*, 1994; *Savage et al.*, 1999; *d'Alessio et al.*, 2005]. Bends, steps, and junctions give rise to accommodating adjacent dip-slip faults that raise mountains and form basins. Thus earthquakes are not limited to the major faults (Figure 1).

[7] The right-lateral Calaveras fault splits off to the east of the San Andreas near the town of Hollister (Figure 1); this junction marks the north end of the creeping segment of the San Andreas fault. The Calaveras fault cuts through a composite of Franciscan Complex, Coast Range Ophiolite, and Great Valley sequence rocks. About 160–170 km of displacement has occurred on the Calaveras fault since slip began in the East Bay fault zone ~8 Ma [*McLaughlin et al.*, 1996].

[8] The Calaveras fault exhibits complex behavior including observed creep at rates between 13 and 16 mm/yr in places [*Galehouse*, 2002] that approach the long-term geologic slip rate of 12–18 mm/yr [*Working Group on California Earthquake Probabilities*, 2003]. While the fault creeps, it also has stick-slip patches evidenced by earthquakes like the 1979 $M = 5.8$ Coyote Lake and 1984 $M = 6.2$ Morgan Hill shocks. The instrumental catalog has 25 $M \geq 4.0$ earthquakes that can be associated with the Calaveras fault segment studied here (Table 1).

3. Catalogs and Methods

[9] On a fault like the Calaveras, that creeps and supports moderate to large earthquakes, it is likely that stress conditions, and by inference, magnitude-frequency distributions, change with time and location. I thus treated time and space independently by first arbitrarily defining subcatalogs along the fault and testing whether timing of $M \geq 4.0$ earthquakes could be associated with temporal *b* value changes. I then assumed *b* value stability over time and systematically examined the whole fault segment to see whether locations of $M \geq 4.0$ earthquakes could be associated with the spatial pattern of *b* values at the time of each $M \geq 4.0$ event.

[10] Earthquakes from the Northern California Seismic Network (NCSN) were assembled into subcatalogs for

Table 1. List of the 25 $M \geq 4.0$ Earthquakes on the Southern Calaveras Fault Used for Forecast Tests in This Study

Date[a]	Magnitude	Latitude	Longitude Depth, km
1970.66	4.0	36.913	−121.471 7.1[b]
1973.76	4.5	37.196	−121.589 6.4[b]
1974.91	5.4	36.920	−121.466 6.1
1974.91	4.4	36.925	−121.468 3.9[b]
1974.92	4.3	37.256	−121.636 6.6
1975.00	4.2	36.933	−121.459 8.7
1975.17	4.2	36.935	−121.461 6.4
1977.05	4.0	36.932	−121.458 8.8
1978.66	4.1	37.356	−121.712 9.2
1979.35	4.4	37.293	−121.663 7.6[b]
1979.60	5.8	37.104	−121.513 8.9
1979.60	4.0	36.996	−121.476 4.3
1984.31	6.2	37.310	−121.679 8.5
1984.74	4.4	37.336	−121.704 7.9
1987.05	4.2	37.160	−121.554 7.1
1988.47	4.1	37.124	−121.526 8.6
1989.00	4.3	37.286	−121.661 7.6
1993.04	5.1	37.018	−121.463 7.9
1993.61	5.0	37.312	−121.679 9.4
1995.70	4.2	37.096	−121.512 8.2
1995.95	4.0	36.976	−121.471 7.6[b]
1996.39	4.9	37.359	−121.723 8.1
1998.45	4.0	37.039	−121.479 8.5
2001.15	4.4	37.333	−121.699 7.8
2006.45	4.7	37.102	−121.492 3.1

[a]Decimal year.
[b]Not used for spatial forecast.

calculating magnitude-frequency distributions along the Calaveras fault. Vertical cylinders with 5-km radii were defined with centers at points along the fault between Hollister at the south end and its junction with the Hayward fault to the north. Earthquakes contained within them were collected into independent subcatalogs (Figure 1). Locations of the cylinder centers were picked arbitrarily along the mapped fault trace with the only consideration being that volumes were adjacent but not overlapping. The mean number of $2.0 \leq M < 4.0$ earthquakes in the subcatalogs was 312 with the largest containing 527 earthquakes and smallest having 97 events (Figure 2). Subcatalogs were treated independently for temporal analysis of magnitude-frequency distributions, and combined together for spatial analysis. No declustering was performed, so there are aftershock decay sequences evident (Figure 2).

[11] To study potential *b* value changes associated with as many $M \geq 4.0$ earthquakes as possible, I wanted to use the whole duration of the instrumental catalog dating to 1968. I therefore limited the calculations to $M \geq 2.0$ earthquakes to guarantee completeness. The retrospective forecast tested whether changes in the distributions of $M < 4.0$ earthquakes could offer any indications of impending $M \geq 4.0$ shocks, so the catalogs were cut off at $M < 4.0$.

[12] Investigators calculate *b* values either with a linear regression to fit the magnitude-frequency trend [e.g., *Abercrombie and Brune*, 1994; *Okal and Romanowicz*, 1994; *Nuannin et al.*, 2005], or via maximum likelihood [e.g., *Utsu*, 1965; *Aki*, 1965; *Enescu and Ito*, 2001; *Schorlemmer et al.*, 2004]. Since there are advocates of both methods, I used weighted least squares regressions and maximum likelihood calculations to conduct the Calaveras fault forecast experiment.

3.1. Linear Regression

[13] Catalog earthquakes were binned in cumulative 0.1 magnitude unit intervals and fit using a linear least squares regression. Groups of 50 events covering variable periods (depending on seismicity rates) were used for temporal analysis. As will be discussed in section 4, significant temporal changes were found in the subcatalogs; a sample size of about 50 events minimized standard deviations of *b* value estimates by trading off number of events versus stability of the distribution over time (Figure 3).

[14] All *b* values calculated with the least squares regression are given with 90% confidence intervals for each calculation. Confidence intervals were calculated for the *b* value slope as

$$b \pm \sqrt{2F_{(2,n-2)}}\sigma_{\overline{b}} \tag{2}$$

where F is Fisher's F distribution, n is the sample size, and $\sigma_{\overline{b}}$ is the standard deviation for the mean b value at a given magnitude M, which is calculated from [*Sachs*, 1984]

$$\sigma_{\overline{b}} = s_{bM}\sqrt{\frac{1}{n} + \frac{\left(M - \overline{M}\right)^2}{Q_M}} \tag{3}$$

where s_{bM} is the residual value at M, $\overline{M}$ is mean magnitude, and Q_M is the sum of the squared residuals.

[15] For spatial analysis, the number of earthquakes at a given location grew with time. Earthquakes of the combined catalog were sampled in 5 km × 5 km rectangular prisms cut on a trend orthogonal to the vertical Calaveras fault surface. Overlapping blocks offset by 2.5-km intervals in depth, and along the Calaveras fault trend were used to calculate spatial variation in *b* values. Volumes not containing at least 50 earthquakes were omitted from the calculations. Binning was by 0.1 magnitude units, *b* values were calculated with a linear least squares technique, and confidence intervals were calculated in the same manner as for the temporal calculations.

3.2. Maximum Likelihood

[16] The maximum likelihood method of *Aki* [1965] and *Utsu* [1965] uses

$$b = \frac{1}{\overline{M} - M_{\min}} \log e \tag{4}$$

where $\overline{M}$ is mean magnitude and $M_{\min}$ is minimum magnitude. According to *Shi and Bolt* [1982] the standard error can be calculated using

$$\sigma(b) = 2.30b^2\sigma\left(\overline{M}\right) \tag{5}$$

where

$$\sigma^2\left(\overline{M}\right) = \sum_{i=1}^{n} \frac{\left(M_i - \overline{M}\right)^2}{n(n-1)} \tag{6}$$

Maximum likelihood calculations were made using the same earthquake sets as described in the discussion of linear

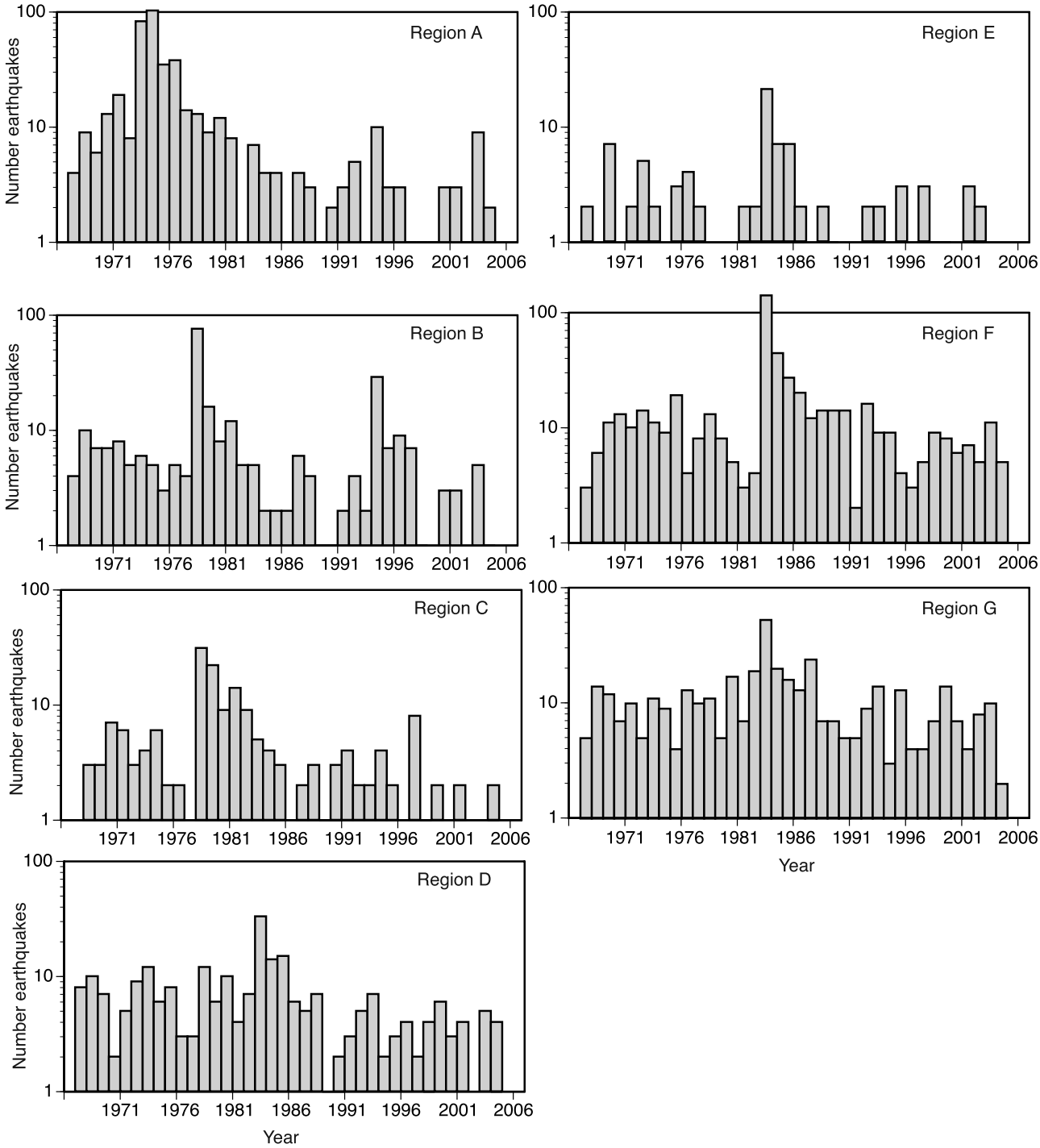

Figure 2. Seismicity rate plots showing the annual number of $2.0 \leq M < 4.0$ earthquakes that occurred within the cylindrical volumes identified in Figure 1. Labels (A–G) correspond to those of Figure 1. The subcatalogs were not declustered, and aftershock sequences can be seen in most subcatalogs.

regression methods. Results acquired using the two methods are compared throughout the analysis.

4. Temporal *b* Value Changes

4.1. Retrospective Test

[17] If the seismic *b* value is inversely proportional to stress [e.g., *Scholz*, 1968: *Main et al.*, 1992; *Amitrano*, 2003; *Schorlemmer et al.*, 2005], then the hypothesis behind forecasting with temporal magnitude-frequency changes is an expectation of lowered *b* value prior to large earthquakes [e.g., *Imoto*, 1991; *Kebede and Kulhánek*, 1994; *Sahu and Saikia*, 1994; *Enescu and Ito*, 2001; *Cao and Gao*, 2002; *Ziv et al.*, 2003; *Nuannin et al.*, 2005]. In this section I discuss whether 24 $M \geq 4.0$ earthquakes that happened within seven 5-km-radius cylindrical volumes centered on

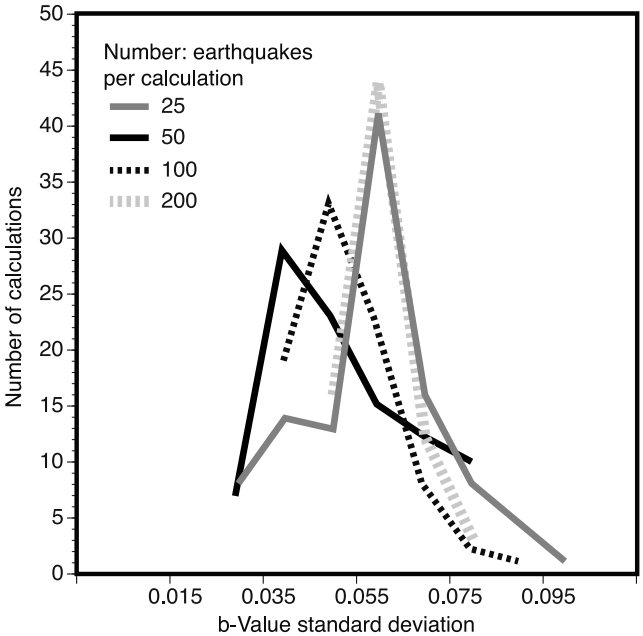

Figure 3. Histograms of standard deviation of *b* value calculations using different numbers of earthquakes ranging from 25 to 200. Earthquakes were gathered with a sliding time window until the desired number was accumulated. The histograms show that standard deviations were minimized when a sample of about 50 earthquakes was used. This results from the offsetting effects of larger sample size reducing misfit, while temporal *b* value variations increase misfit when longer time widows were used.

the Calaveras fault were associated with significant changes in *b* value before their occurrence in a retrospective test. A M = 4.7 earthquake struck the Calaveras fault after the analysis was complete, enabling a prospective test, which is described separately.

[18] Of seven regions where subcatalogs of Calaveras fault earthquakes were culled (labeled A–G on Figure 1), five showed temporal changes in *b* value in excess of 90% confidence, and two did not (Figures 4 and 5). In the subcatalogs there were periods of *b* value stability that lasted ~15–25 years. There were no clear similarities in temporal *b* value patterns between regions. In some cases, *b* value perturbations followed $M \geq 4.0$ shocks such as in region A (Figure 5). These were likely related to aftershock sequences because temporal changes in excess of 90% confidence intervals initiated immediately after, rather than before $M \geq 4.0$ events. For example, in region C (Figure 4), beginning in about 1982, the *b* value began dropping progressively with time from ~1.1 down to ~0.8 in 1990. There was an accompanying seismicity rate decline that happened during that interval (Figure 2), probably resulting from aftershock decay from the 1979 M = 5.8 Coyote Lake earthquake. Temporal *b* value changes associated with aftershock sequences seems to support the idea that *b* values are related to stress changes [*Scholz*, 1968; *Main et al.*, 1992; *Amitrano*, 2003; *Ziv et al.*, 2003; *Schorlemmer et al.*, 2005], since aftershocks are thought to result from stress changes caused by main shocks [e.g., *Stein*, 1999].

[19] It is difficult to identify any precursory temporal *b* value changes before $M \geq 4.0$ earthquakes, especially given the tendency for the trends to look different depending on calculation method. For example in region D, a *b* value decline is evident after 1998 when calculated with the least squares method, but is absent on the maximum likelihood curve (Figure 5). More instructive is an examination of *b* values immediately preceding all 24 $M \geq 4.0$ earthquakes in the catalog together (Figure 6). No consistent pattern of either low or high *b* values is revealed prior to rupture times. Three $M \leq 4.0$ events occurred when *b* values were significantly greater than the mean of b = 0.95, 4 happened when *b* values were less than the mean, and 17 occurred when *b* values were indistinguishable form the mean. No significant relationship was found between *b* values and earthquake magnitude (Figure 6a) or between *b* values and catalog time (Figure 6b).

[20] Since the Calaveras fault is known to creep, a possibility exists that slow earthquakes might cause stress changes on the fault, and by extension, *b* value changes as well. Two sites where creep has been monitored are coincident with studied subregions along the fault, at Hollister and Coyote Ranch (Figure 1). At each site there was one significant change in creep rate, an acceleration during and after the 1979 M = 5.8 Coyote Lake earthquake observed at the Coyote Ranch site (subregion C), and slowed creep at Hollister following the 1989 M = 7.1 Loma Prieta earthquake [*Galehouse*, 2002] (Figure 7). It is possible to associate a *b* value anomaly with the Coyote Ranch rate change (Figure 7), but *b* values in the studied subregion closest to the Hollister site (subregion A) were unchanged during the 1989–1994 interval of slowed creep (Figure 5).

[21] To summarize, the retrospective test using temporal *b* value changes to forecast $M \geq 4.0$ earthquakes on the Calaveras fault was not successful. Some events were consistent with the hypothesis of lowered *b* values prior to their occurrence, but an equal number were not (Figure 6), and a majority occurred when *b* values were indistinguishable from the overall mean. Rupture surfaces of M~4.0 earthquakes are small compared with the 5-km-radius cylinders required to make temporal *b* value calculations. It is therefore possible that temporal variations were averaged over too large a region, although no apparent relationship was evident between $M \geq 5.0$ shocks and *b* values at the times of their ruptures either (Figure 6a).

4.2. The 15 June 2006 M = 4.7 Earthquake

[22] After the temporal and spatial *b* value analysis for the Calaveras fault was completed, and as this paper was being written, a M = 4.7 shock struck the Calaveras fault. Since all calculations were completed before its occurrence, this event can be used in a prospective forecast test rather than retrospective like the other $M \geq 4.0$ events in the catalog. The 15 June 2006 event was located closest to region C (Figure 1). If temporal *b* value changes in region C were used to forecast $M \geq 4.0$ earthquakes, then the 15 June shock was not expected. Calculated *b* values late in the catalog for region C showed higher than mean *b* values with broad uncertainty (Figures 4 and 5), because the seismicity rate was low (Figure 2). This temporal forecast failure is consistent with the retrospective temporal forecast test for

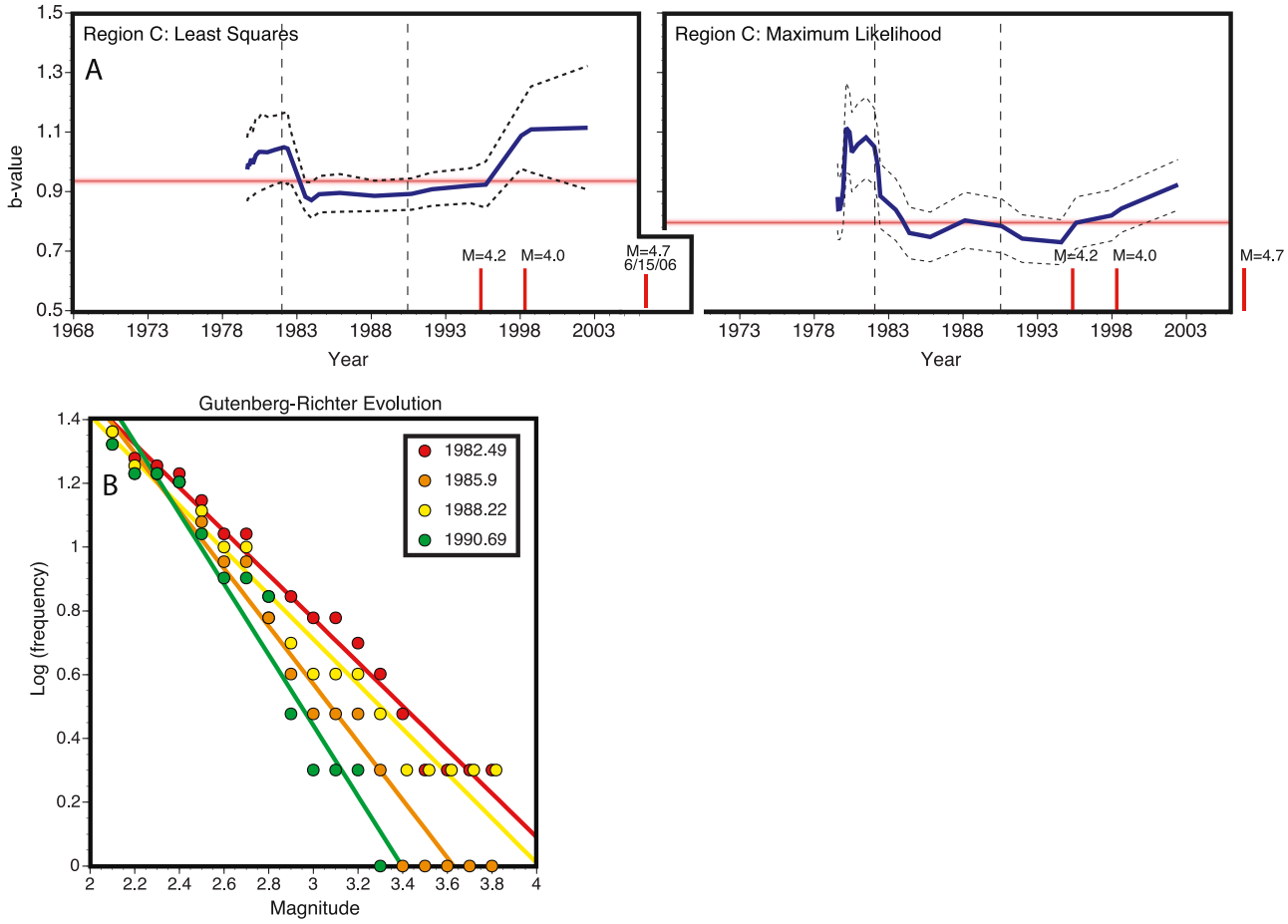

Figure 4. (a) Example plot of *b* value versus time from subcatalog C (see Figure 1 for location) calculated with least squares and maximum likelihood methods. Dashed lines show 90% confidence intervals on the *b* value calculations. Labeled markers on the horizontal axes show the times and magnitudes of $M \geq 4.0$ earthquakes that occurred within the subcatalog. The horizontal lines represent attempts to fit constant *b* values within the 90% confidence intervals. Beginning about 1982 the *b* value began to drop from ~1.1 to ~0.8 by 1990. (b) Individual linear fits to the data for the 1982–1990 period, where a gradual decrease in slope is evident. While the *b* value dropped over this period, no $M \geq 4.0$ earthquakes occurred. The most likely explanation appears to be a seismicity rate reduction over the interval (Figure 2), as the rate of aftershocks from the 1979 $M = 5.8$ Coyote Lake earthquake decayed.

the Calaveras fault. In section 5 I discuss results from retrospective and prospective spatial forecast tests.

5. Spatial *b* Value Changes

5.1. Retrospective Test

[23] If the seismic *b* value is inversely proportional to stress on a fault, and the *b* value is stable over time, then its spatial distribution might identify fault areas where earthquakes will most likely happen [e.g., *Westerhaus et al.*, 2002; *Schorlemmer et al.*, 2003; *Wyss et al.*, 2004; *Schorlemmer et al.*, 2004; *Wyss and Stefansson*, 2006]. In section 4 I showed temporal *b* values changes that were significant at 90% confidence. However, in many cases these changes were associated with aftershock sequences, and were dependent on calculation method. Lengthy (~15–25 years) periods of stationary *b* values were calculated. Further, temporal *b* value changes did not portend $M \geq 4.0$ earthquakes. In this section I assume that *b* values can be treated as stationary in time during interseismic periods with a goal of testing whether spatial *b* value variation is an effective forecast tool for $M \geq 4.0$ events.

[24] As discussed in section 2, there was better spatial resolution than in the temporal forecast test because it was possible to use much more of the catalog than just 50 events. Therefore smaller (5 km × 5 km), overlapping volumes could be used to collect earthquakes for magnitude-frequency distributions with an apparent resolution of 2.5 km × 2.5 km projected onto a fault-parallel cross section (Figure 8). To make a quantitative test of the spatial forecast, a *b* value at a cell containing each $M \geq 4.0$ earthquake hypocenter was compared to the distribution of *b* values along the entire fault zone. If a hypocentral *b* value was less than the mean value at 90% confidence, then the spatial forecast was considered a success, whereas if the hypocentral *b* value exceeded the mean, then the forecast was regarded as a failure. Otherwise, the test was considered inconclusive. Of the 24 $M \geq 4.0$ events in the

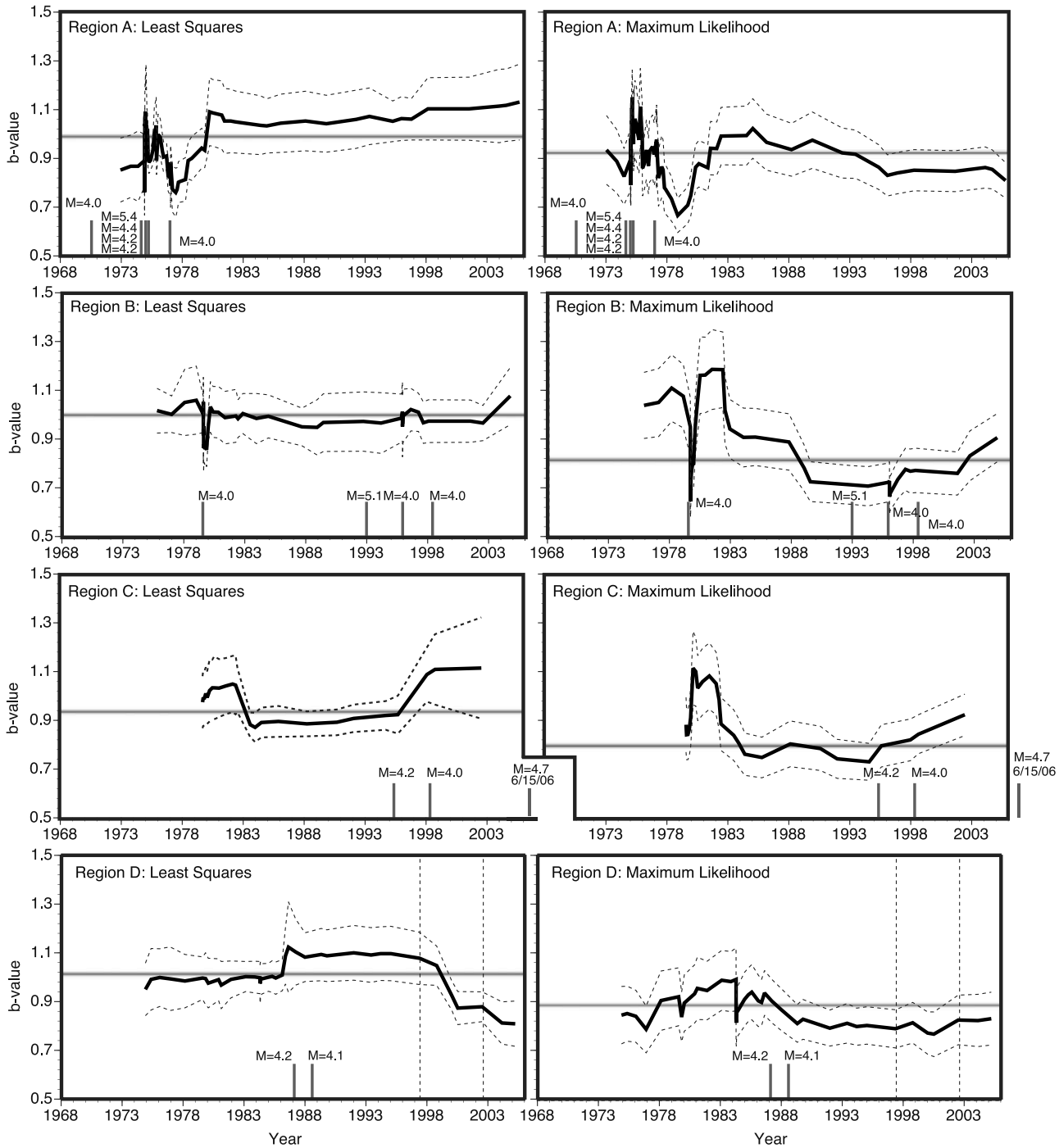

Figure 5. Temporal changes in *b* value for subcatalogs A–G (see Figure 1 for locations). Plot characteristics are the same as described for Figure 4a. (left) Calculations made with a least squares technique, and (right) equivalent maximum likelihood calculations. In five of these regions it was not possible to fit a constant *b* value over the catalog duration within the 90% confidence intervals. There was not any apparent correlation with temporal *b* value changes and $M \geq 4.0$ earthquake occurrence with the exception of some aftershock sequences. In most of the regions, there were long periods (~15–25 years) of constant *b* value at 90% confidence.

retrospective catalog, 19 could be investigated, while 5 lacked enough prior earthquakes to calculate a *b* value.

[25] Figures 9 and 10 show spatial *b* value distributions made for times just before each of the 20 $M \geq 4.0$ earthquakes in the catalog (19 retrospective, 1 prospective) using least squares and maximum likelihood calculations. For each $M \geq 4.0$ earthquake, lines were drawn at *b* value distribution means and hypocenter values for comparison. The distribution shapes change over time, which is likely the effect of the growing number of catalog events with time, and

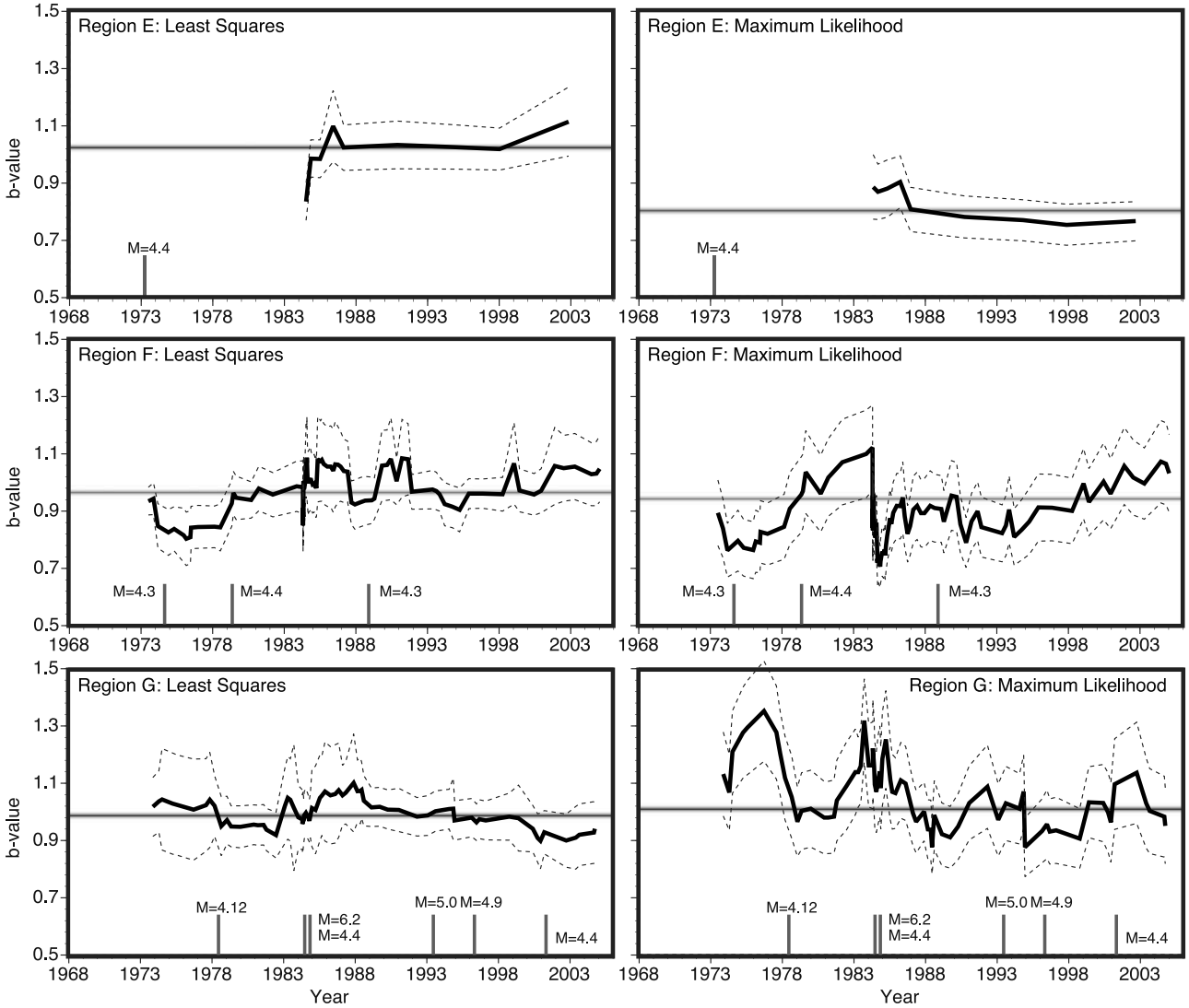

Figure 5. (continued)

possibly effects of the $M \geq 4.0$ earthquakes on stress (suggested to affect *b* values by *Ziv et al.* [2003]).

[26] When differences between hypocenter *b* values and mean *b* values were compiled together, the results were as follows: using a least squares calculation, 10 of 19 tested events were inconclusive because differences between distribution means and hypocentral *b* values were less than the 90% confidence intervals. Of the remaining nine events, seven occurred at places where *b* values were less than the distribution mean at 90% confidence, and two occurred where the *b* values were higher than the mean (Figure 11). If maximum likelihood calculations were used, 12 of 19 tested events were inconclusive. Of the remaining seven events, six occurred at places where *b* values were less than the distribution mean at 90% confidence, and one occurred where the *b* values were higher than the mean (Figure 12). Results depended on *b* value calculation methods; only 4 of the 19 events were found to be significantly less than the mean regardless of calculation method. None of the *b* values significantly greater than the mean were common to both methods. No functional relationship was evident between hypocenter *b* value difference and either earthquake magnitude or catalog time (Figures 11 and 12).

[27] In summary, the retrospective forecast test could not rule out the hypothesis that low *b* value regions are more likely to contain $M \geq 4.0$ earthquake hypocenters than high *b* value regions. When it was possible to distinguish significant spatial *b* value variation, earthquakes were at least 4 times more likely to occur where *b* values were less than the mean than where *b* values exceeded the mean. However, the most frequent outcome was that $M \geq 4.0$ earthquakes happened at places where *b* values were indistinguishable from the mean. Only 4 of 19 $M \geq 4.0$ shocks occurred where *b* values were calculated to be significantly less than the mean value using both the maximum likelihood and least squares method. Thus spatial *b* value variation might be a useful forecast tool, but resolution is poor, even on seismically active faults like the Calaveras.

5.2. The 15 June 2006 $M = 4.7$ Earthquake

[28] The spatial *b* value plots shown in Figure 8 were made prior to the occurrence of the 15 June 2006 $M = 4.7$

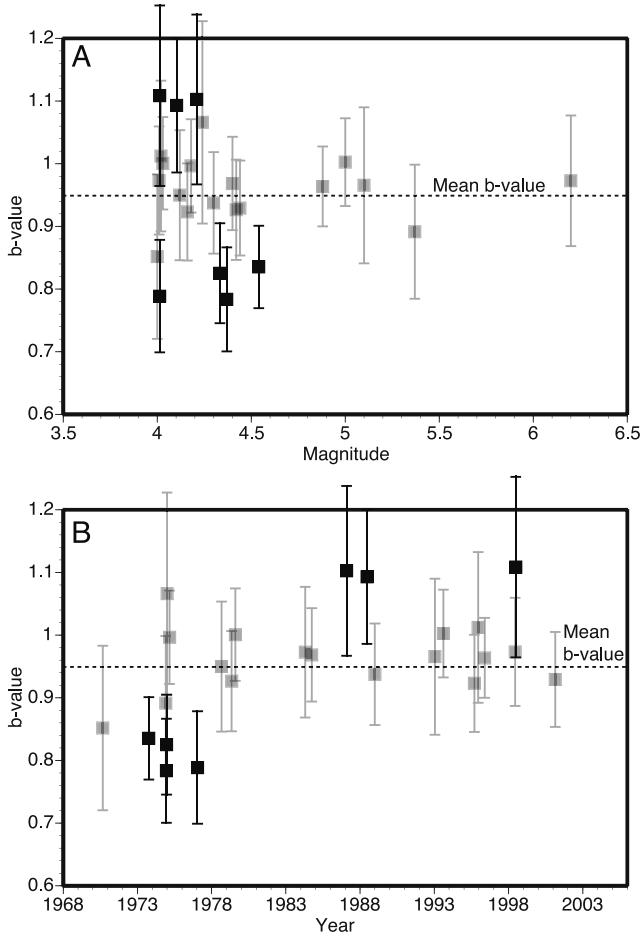

Figure 6. Plots of *b* value from the seven subcatalogs at the times of 24 $M \geq 4.0$ earthquakes that occurred within them. Most of the earthquakes (17) happened when *b* values were indistinguishable (at 90% confidence) from the mean value of 0.95, while 3 happened when *b* values were greater than the mean, and 4 when *b* values were less than the mean. (a) The *b* values at $M \geq 4.0$ earthquake times are plotted against magnitude, and (b) *b* values plotted against catalog time. In neither case is there a readily apparent relationship.

earthquake and were calculated with all catalog events up to the end of 2005. The 15 June earthquake location was added to the cross section as shown by the stars in Figure 8. In addition, spatial *b* value distributions were added to Figures 9 and 10. The 15 June event happened at a location where *b* values were significantly lower than the mean using a least squares calculation. However, when a maximum likelihood calculation was used, the *b* value at the 15 June hypocenter was within the 90% confidence interval of the mean. Thus the spatial *b* value forecast as set up in this experiment cannot be considered a successful indicator of the 15 June 2006 $M = 4.7$ earthquake.

6. Conclusions

[29] Two forecast experiments were conducted using seismic *b* values calculated with $2.0 \leq M < 4.0$ earthquakes: a temporal forecast of 25 $M \geq 4.0$ Calaveras fault earthquakes, and a spatial forecast using 20 of the same set of events. The hypotheses tested were that $M \geq 4.0$ earthquakes might be expected either at times or locations of low *b* value, based on laboratory and theoretical suggestions that low *b* values imply high stress. Results were mixed. The temporal forecast failed; despite identification of significant (at 90% confidence) time variation in the *b* value within 5-km-radius vertical cylinders along the fault, no relationship between earthquake occurrence and temporal *b* value differences was identified. It is possible that crustal volumes of sufficient size to collect enough events for temporal *b* value variations were too large relative to rupture areas of $M \sim 4.0$ shocks. However, no temporal *b* value relationship was identified with rupture times among the five $M = 5.0$ to $M = 6.2$ shocks in the catalogs. I thus conclude that temporal *b* value variations are not useful in forecasting south Calaveras fault earthquakes.

[30] Since significant temporal *b* value changes were calculated, it is not strictly true that the spatial *b* value distribution was stationary over time on the Calaveras fault. However, the *b* value distribution was stable for lengthy

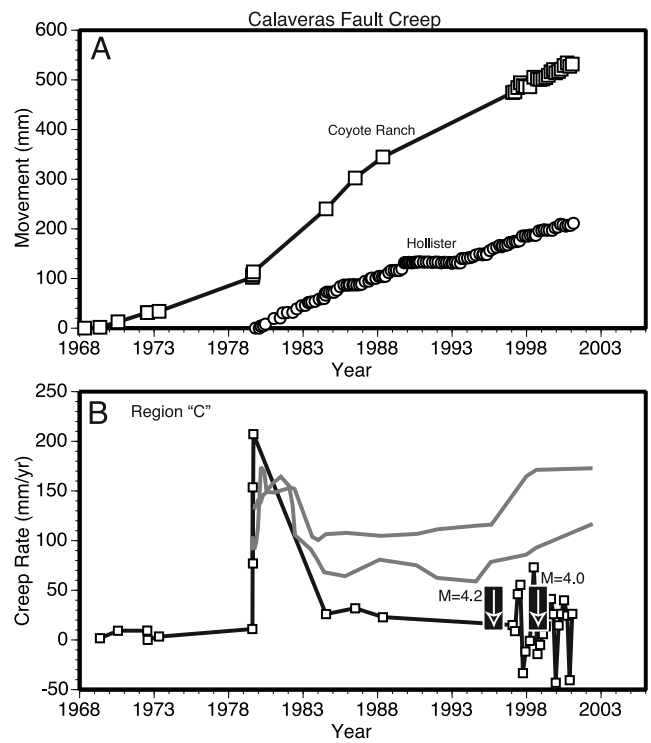

Figure 7. Plots of (a) creep versus time and (b) creep rate versus time from two long-term monitoring sites on the Calaveras fault [*Galehouse*, 2002] (see Figure 1 for site locations). No relationship between creep or creep rate was evident in *b* value changes calculated for subcatalog A, which was closest to the Hollister site, and which showed no significant temporal *b* value variation despite a clear cessation of creep beginning in 1989 after the Loma Prieta earthquake. However, subcatalog C showed a significant *b* value change (shown as gray lines in Figure 7b) at about the same time that creep accelerated after the 1979 $M = 5.8$ Coyote Lake earthquake. Both the creep episode and aftershock activity were associated with the Coyote Lake event making it difficult to resolve any association.

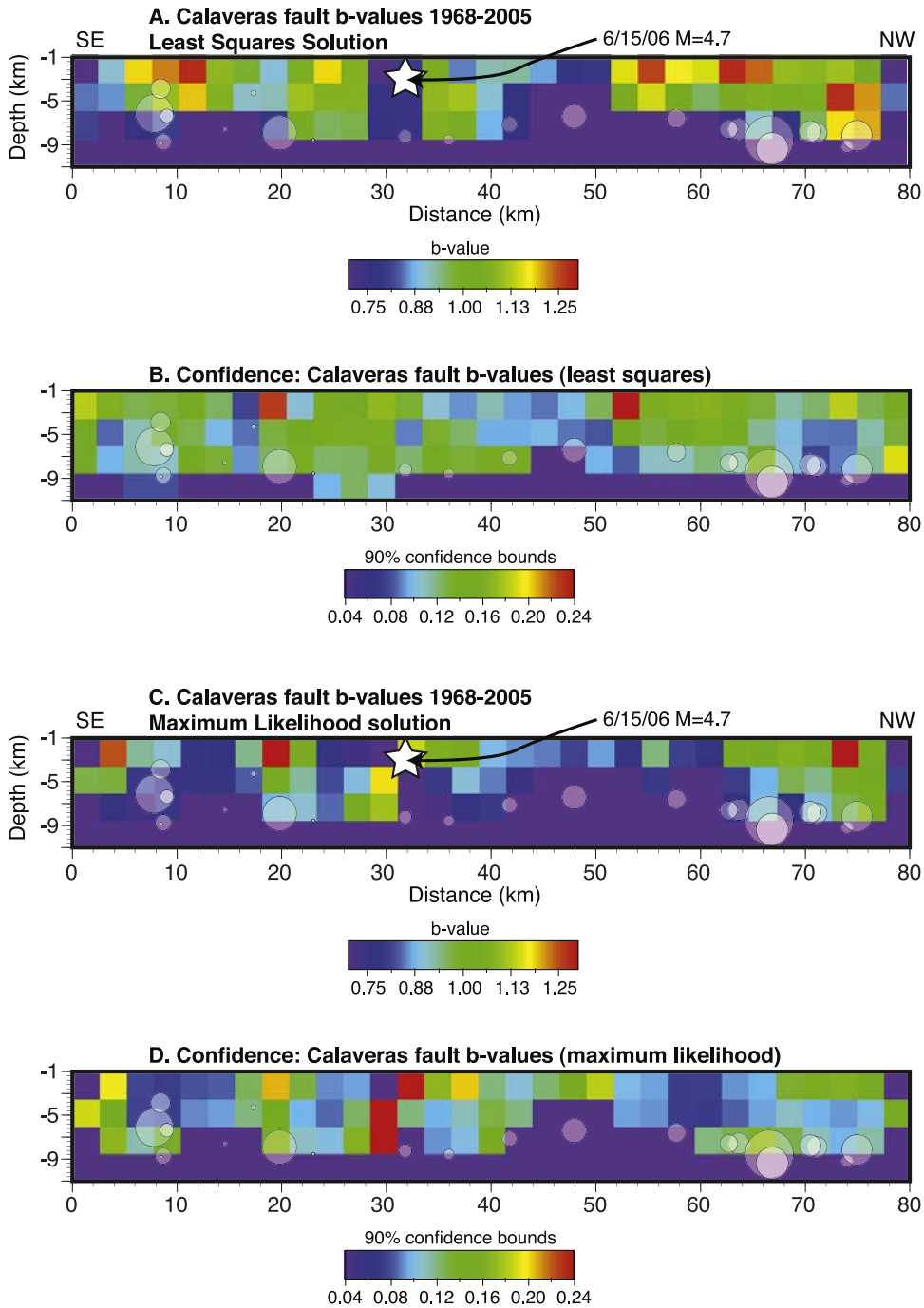

Figure 8. (a) Spatial distribution of *b* values on the south Calaveras fault at the end of 2005 calculated using a least squares regression. (b) Spatial distribution of 90% confidence bounds corresponding to *b* values shown in Figure 8a. (c) Spatial distribution of *b* values calculated by maximum likelihood; (d) associated 90% confidence intervals. The location of the 15 June 2006 $M = 4.7$ earthquake that occurred just as this study was completed is shown with white stars. Circles show all $M \geq 4.0$ earthquake locations.

periods (~15–25 years) in most cases. When temporal stability was assumed, I could not rule out the hypothesis that $M \geq 4.0$ earthquakes should nucleate on parts of the Calaveras fault that had low *b* values. Of 19 earthquakes that could be included in the retrospective forecast, at least 10 were inconclusive, 6 to 7 (depending on calculation method) were associated with regions of *b* value significantly lower than the mean (at 90% confidence), while 1 to 2 happened in regions significantly higher then the mean. A $M = 4.7$ earthquake struck just as this study was being finalized (15 June 2006); this event was consistent with the conclusions from the retrospective forecast in that it was not associated with a temporal *b* value low. Spatial forecasting of this event was inconclusive; the event occurred where a

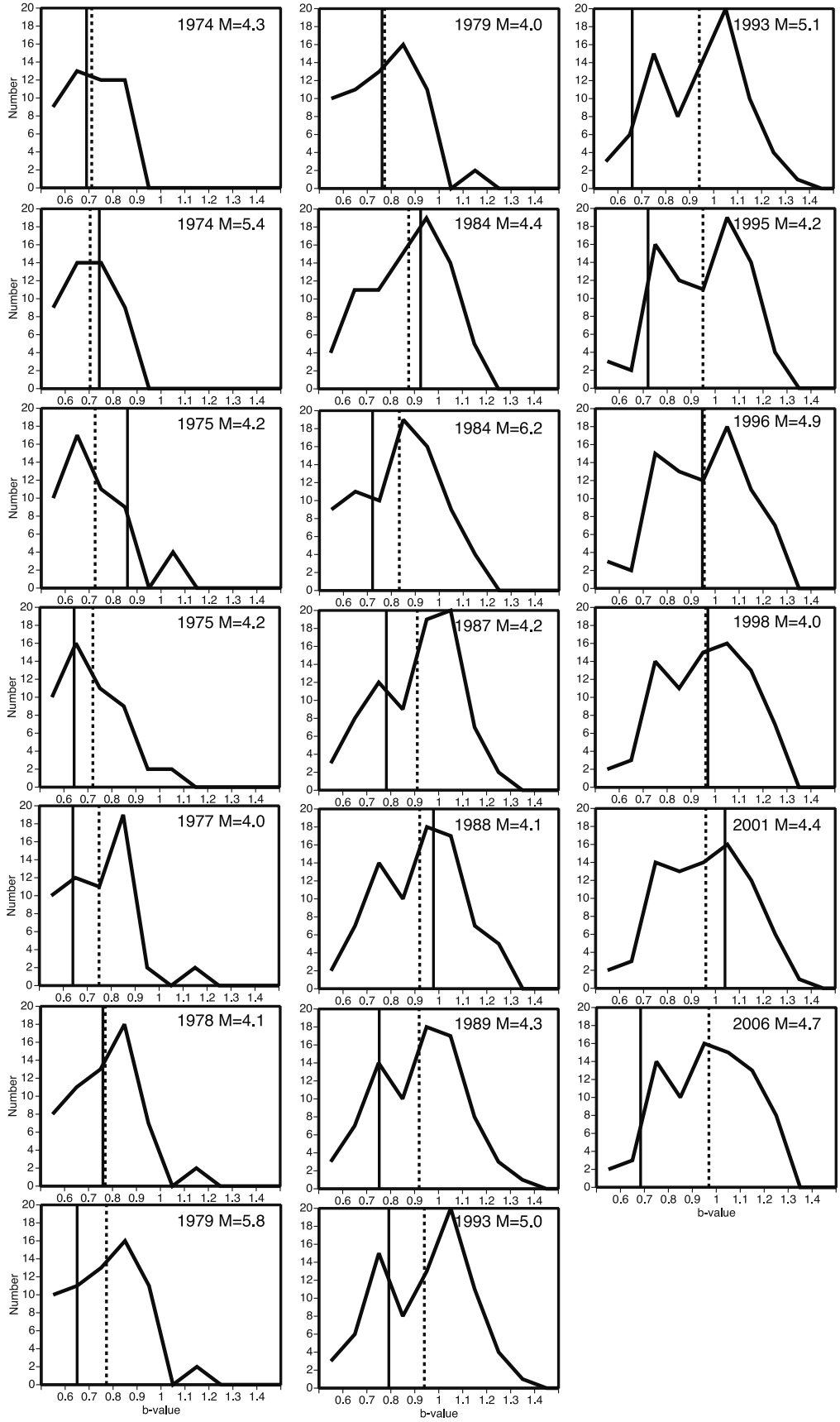

Figure 9. Distributions of spatial b values calculated at the times of 20 $M \geq 4.0$ earthquakes on the Calaveras fault using a least squares regression. Dashed vertical lines show distribution means, and solid vertical lines show b values at cells containing $M \geq 4.0$ earthquake hypocenters.

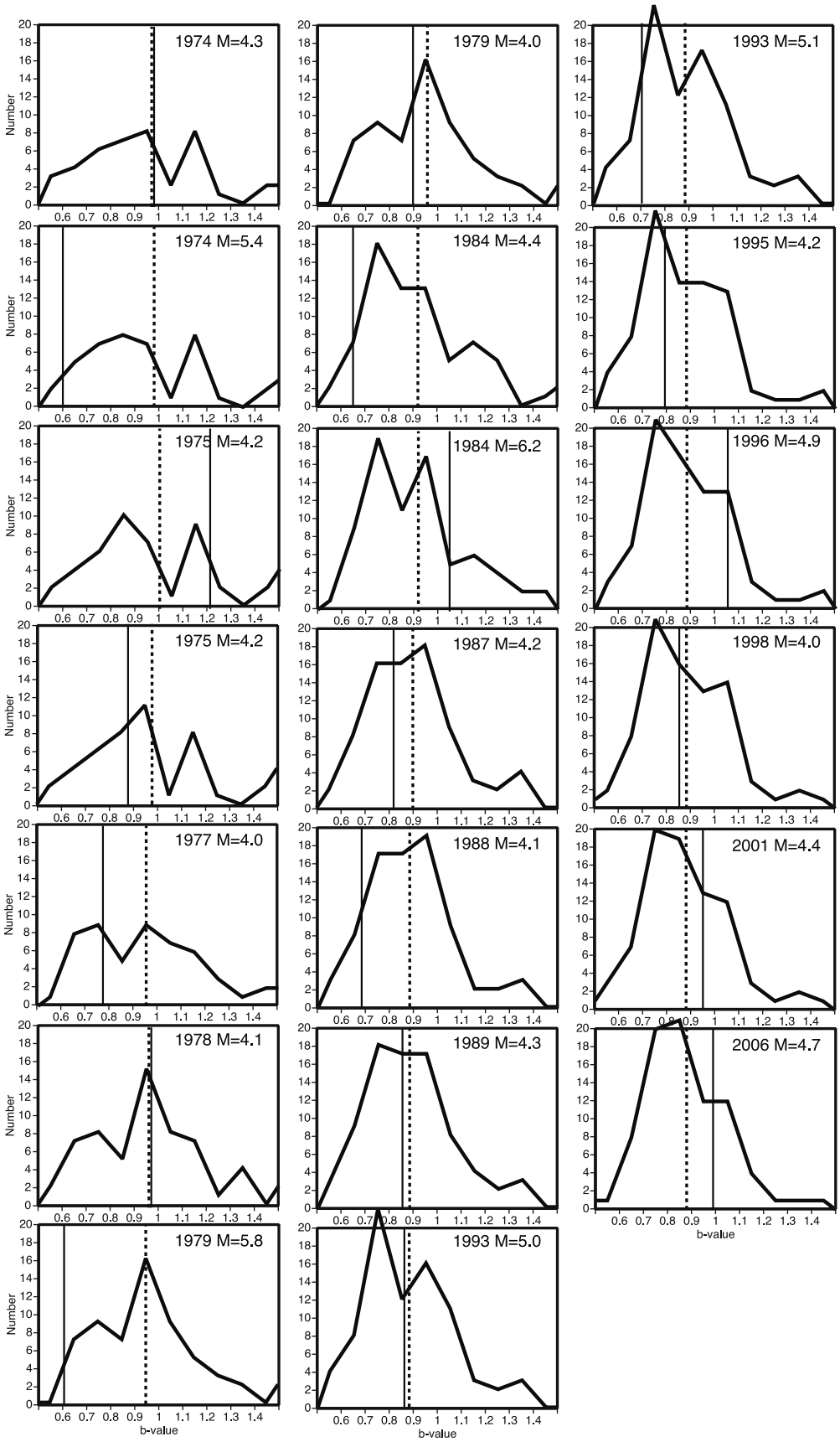

Figure 10. Distributions of spatial *b* values calculated at the times of 20 $M \geq 4.0$ earthquakes on the Calaveras fault calculated by maximum likelihood. Dashed vertical lines show distribution means and solid vertical lines show *b* values at cells containing $M \geq 4.0$ earthquake hypocenters.

spatial *b* value calculation showed low values using a least squares technique but was within the 90% confidence interval of the mean when a maximum likelihood calculation was used.

[31] To the extent that these results might be extended to other fault zones, they tend to be most consistent with studies that have concluded temporally stationary *b* values with spatial variation portending future seismicity [e.g., *Abercrombie and Brune*, 1994; *Westerhaus et al.*, 2002; *Schorlemmer et al.*, 2003; *Wyss et al.*, 2004; *Schorlemmer et al.*, 2004; *Wyss and Stefansson*, 2006].

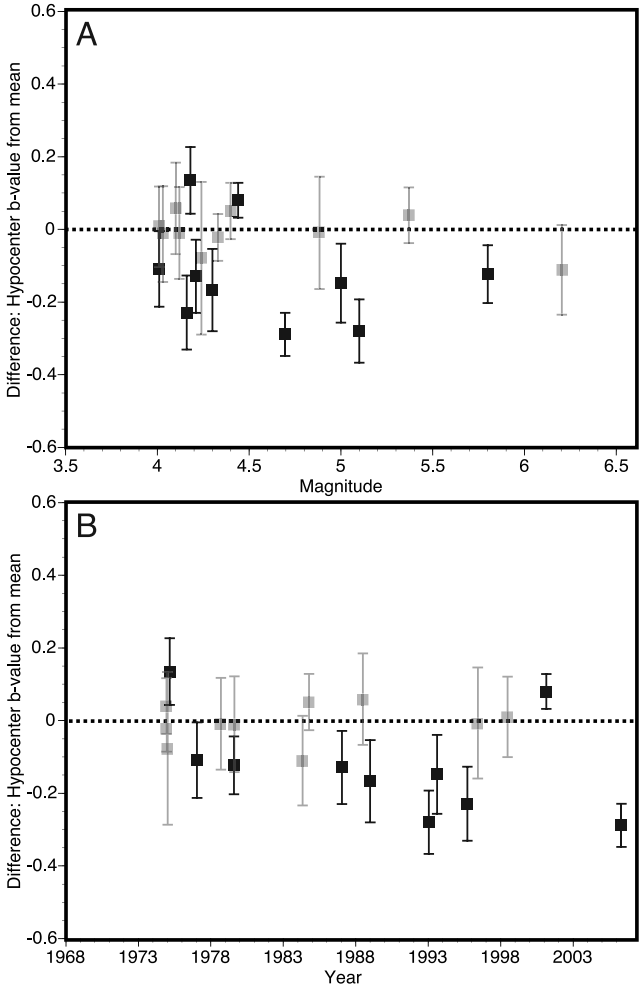

Figure 11. Plots of the differences between $M \geq 4.0$ earthquake hypocenter *b* values (least squares method) and spatial distribution means shown in Figure 9. Error bars show 90% confidence intervals for each *b* value calculation. If the difference between hypocenter *b* values and distribution means exceeded the 90% confidence bounds and was less than zero, then the result was interpreted as consistent with the hypothesis that earthquakes are expected at locations with lower *b* values. Conversely if the difference was greater than zero, then the result was interpreted as inconsistent with the hypothesis. Eight $M \geq 4.0$ earthquakes were interpreted as consistent with the spatial *b* value hypothesis, 2 were not, and 10 were too close to the mean value to tell. Results plotted (a) against magnitude and (b) against catalog time. No relationship is apparent in either case. Lighter symbols are used for inconclusive events.

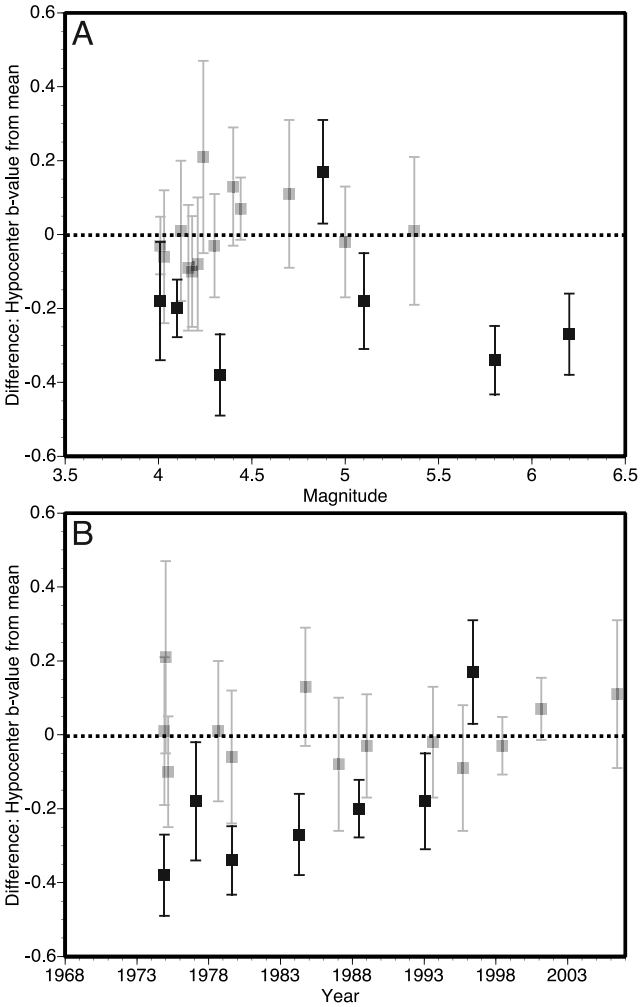

Figure 12. Plots of the differences between $M \geq 4.0$ earthquake hypocenter *b* values (maximum likelihood) and spatial distribution means shown in Figure 10. Error bars show 90% confidence intervals for each *b* value calculation. Six $M \geq 4.0$ earthquakes were interpreted as consistent with the spatial *b* value hypothesis, 1 was not, and 13 were too close to the mean value to tell. Results plotted (a) against magnitude and (b) against catalog time. No relationship is apparent in either case. Lighter symbols are used for inconclusive events.

[32] **Acknowledgments.** I thank Bogdan Enescu, an anonymous reviewer, the Associate Editor, and the AGU editorial staff for improving this paper.

References

Abercrombie, R. E., and J. N. Brune (1994), Evidence for a constant b-value above magnitude 0 in the southern San Andreas, San Jacinto and San Miguel fault zones, and at the Long Valley caldera, California, *Geophys. Res. Lett.*, *21*, 1647–1650.

Aki, K. (1965), Maximum likelihood estimate of b in the formula log N = a – bM and its confidence limits, *Bull. Earthquake Res. Inst. Univ. Tokyo*, *43*, 237–239.

Amitrano, D. (2003), Brittle-ductile transition and associated seismicity: Experimental and numerical studies and relationship with the *b* value, *J. Geophys. Res.*, *108*(B1), 2044, doi:10.1029/2001JB000680.

Cao, A., and S. S. Gao (2002), Temporal variation of seismic *b*-values beneath northeastern Japan island arc, *Geophys. Res. Lett.*, *29*(9), 1334, doi:10.1029/2001GL013775.

d'Alessio, M. A., I. A. Johanson, R. Bürgmann, D. A. Schmidt, and M. H. Murray (2005), Slicing up the San Francisco Bay Area: Block kinematics and fault slip rates from GPS-derived surface velocities, *J. Geophys. Res.*, *110*, B06403, doi:10.1029/2004JB003496.

DeMets, C., R. G. Gordon, D. F. Argus, and S. Stein (1994), Effect of recent revisions to the geomagnetic reversal time scale on estimates of current plate motions, *Geophys. Res. Lett.*, *21*, 2191–2194.

Enescu, B., and K. Ito (2001), Some premonitory phenomena of the 1995 Hyogo-Ken Nanbu (Kobe) earthquake: seismicity, b-value and fractal dimension, *Tectonophysics*, *338*, 297–314.

Galehouse, J. S. (2002), Data from theodolite measurements of creep rates on San Francisco Bay Region faults, California: 1979–2001, *U.S. Geol. Surv. Open File Rep.*, *02–225*, 94 pp.

Gutenberg, B., and C. R. Richter (1954), Magnitude and energy of earthquakes, *Ann. Geofis.*, *9*, 1–15.

Imoto, M. (1991), Changes in the magnitude-frequency b-value prior to large (≥6.0) earthquakes in Japan, *Tectonophysics*, *193*, 311–325.

Ishimoto, M., and K. Iida (1939), Observations sur les seismes enregistres par le microseimographe construit dernierement (in Japanese with French abstract), *Bull. Earthquake Res. Inst. Univ. Tokyo*, *17*, 443–478.

Kanamori, H., and T. Heaton (2000), Microscopic and macroscopic physics of earthquakes, in *GeoComplexity and the Physics of Earthquakes*, *Geophys. Monogr. Ser.*, vol. 120, edited by J. B. Rundle, D. L. Turcotte, and W. Klein, pp. 147–163, AGU, Washington, D. C.

Kebede, F., and O. Kulhánek (1994), Spatial and temporal variations of b-values along the East African rift system and the southern Red Sea, *Phys. Earth Planet. Inter.*, *83*, 249–264.

Main, I. G., P. G. Meredith, and P. R. Sammonds (1992), Temporal variations in seismic event rate and b-values from stress corrosion constitutive laws, *Tectonophysics*, *211*, 233–246.

McGarr, A. (1999), On relating apparent stress to the stress causing earthquake fault slip, *J. Geophys. Res.*, *104*, 3003–3011.

McLaughlin, R. J., W. V. Sliter, D. H. Sorg, P. C. Russell, and A. M. Sarna-Wojcicki (1996), Large-scale right-slip displacement on the East San Francisco Bay Region fault system, California: Implications for location of late Miocene to Pliocene Pacific plate boundary, *Tectonics*, *15*, 1–18.

Nuannin, P., O. Kulhanek, and L. Persson (2005), Spatial and temporal *b* value anomalies preceding the devastating off coast of NW Sumatra earthquake of December 26, 2004, *Geophys. Res. Lett.*, *32*, L11307, doi:10.1029/2005GL022679.

Okal, E. A., and B. A. Romanowicz (1994), On the variation of b-values with earthquake size, *Phys. Earth Planet. Inter.*, *87*, 55–76.

Sachs, L. (1984), *Applied Statistics*, 707 pp., Springer, New York.

Sahu, O. P., and M. M. Saikia (1994), The *b* value before the 6th August, 1988 India-Myanmar border region earthquake: A case study, *Tectonophysics*, *234*, 349–354.

Savage, J. C., J. L. Svarc, and W. H. Prescott (1999), Geodetic estimates of fault slip rates in the San Francisco Bay area, *J. Geophys. Res.*, *104*, 4995–5002.

Scholz, C. H. (1968), The frequency-magnitude relation of microfracturing in rock and its relation to earthquakes, *Bull. Seismol. Soc. Am.*, *58*, 399–415.

Scholz, C. H. (2002), *The Mechanics of Earthquakes and Faulting*, Cambridge Univ. Press, New York.

Schorlemmer, D., G. Neri, S. Wiemer, and A. Mostaccio (2003), Stability and significance tests for *b*-value anomalies: Example from the Tyrrhenian Sea, *Geophys. Res. Lett.*, *30*(16), 1835, doi:10.1029/2003GL017335.

Schorlemmer, D., S. Wiemer, and M. Wyss (2004), Earthquake statistics at Parkfield: 1. Stationarity of *b* values, *J. Geophys. Res.*, *109*, B12307, doi:10.1029/2004JB003234.

Schorlemmer, D., S. Weimer, and M. Wyss (2005), Variations in earthquake-size distribution across different stress regimes, *Nature*, *437*, 539–542, doi:10.1038/nature04094.

Shi, Y., and B. A. Bolt (1982), The standard error of the magnitude-frequency *b* value, *Bull. Seismol. Soc. Am.*, *72*, 1677–1687.

Stein, R. S. (1999), The role of stress transfer in earthquake occurrence, *Nature*, *402*, 605–609.

Utsu, T. (1965), A method for determining the value of b in a formula log n = a − bM showing the magnitude-frequency relation for earthquakes, *Geophys. Bull. Hokkaido Univ.*, *13*, 99–103.

Westerhaus, M., M. Wyss, R. Yilmaz, and J. Zschau (2002), Correlating variations of *b* values and crustal deformation during the 1990's may have pinpointed the rupture initiation of the M_w = 7.4 Izmit earthquake of 1999 August 17, *Geophys. J. Int.*, *148*, 139–152.

Working Group on California Earthquake Probabilities (2003), Earthquake probabilities in the San Francisco Bay Region: 002–031, *U.S. Geol. Surv. Open File Rep, 03–214*, 235 pp.

Wyss, M., and R. Stefansson (2006), Nucleation points of recent mainshocks in southern Iceland mapped by b-values, *Bull. Seismol. Soc. Am.*, *96*, 599–608, doi:10.1785/0120040056.

Wyss, M., C. G. Sammis, and R. M. Nadeau (2004), Fractal dimension and b-value on creeping and locked patches of the San Andreas fault near Parkfield, California, *Bull. Seismol. Soc. Am.*, *94*, 410–421.

Ziv, A., A. M. Rubin, and D. Kilb (2003), Spatiotemporal analyses of earthquake productivity and size distribution: observations and simulations, *Bull. Seismol. Soc. Am.*, *93*, 2069–2081.

T. Parsons, U.S. Geological Survey, 345 Middlefield Road, MS 999, Menlo Park, CA 94025, USA. (tparson@usgs.gov)